33rd Annual International Conference of the IEEE EMBS
Boston, Massachusetts USA, August 30 - September 3, 2011

Assessing Electrical Impedance Alterations in Spinal Muscular Atrophy via the Finite Element Method

Mina Jafarpoor, BS, Andrew J. Spieker, BS, Jia Li, PhD, Minhee Sung, BS, Basil T. Darras, MD, and Seward B. Rutkove, MD

Abstract— **Electrical impedance myography (EIM) is a surface-based, non-invasive technique of evaluation of muscle health, involving the application of high frequency, low-amplitude current to the skin over a muscle of interest. Results from a previous animal study suggest that the finite element method can relate disease-induced changes in electrical properties of the muscle to alterations in surface impedance measurements; however, whether such an approach will prove useful in human models is uncertain. Therefore, to further investigate this question, we have created a single finite element model of the human biceps muscle using data from one healthy subject and one with spinal muscular atrophy (SMA), each of whom had comparable age, limb girth, muscle size, and subcutaneous fat thickness. Since healthy human tissue was unavailable, permittivity and conductivity measurements were obtained from five healthy and five advanced amyotrophic lateral sclerosis rat gastrocnemius muscles immediately after sacrifice; their data were input into the human biceps model and the expected surface voltages calculated. We then compared the results of this model to the actual surface EIM data for both individuals. Although the actual resistance and reactance values varied and the peak values were displaced, the resulting maximum phase predicted by the model approximated that obtained with surface recordings. These results support that alterations in the primary characteristics of muscle impact the surface impedance measurements in meaningful and likely predictable ways.**

I. Introduction

Spinal muscular atrophy (SMA) is a relatively common neuromuscular disease in children, affecting more than 1 in 10,000 live births [1]. Several trials assessing potential treatments for SMA are ongoing or are being planned [2]. However, currently used tools to track disease progression (biomarkers) are lacking in certain respects. One specific challenge of SMA is that the disease is slowly progressive or possibly static; thus finding a change over an acceptable period of time (e.g., 1 year or less) is challenging [3, 4]. Moreover, the disease may be most progressive in younger children in whom measures such as strength or functional testing cannot be performed. Other methods, such as motor unit number estimation (MUNE) [5] are time- consuming to perform and are not well tolerated by many children.

Electrical impedance myography (EIM) is a non-invasive technique used to evaluate muscle health through application of high-frequency, low-intensity current to the skin over a discrete area of muscle via surface electrodes [6]; the impedance parameters resistance (R) and reactance (X) are determined from the input current and the resulting voltage. Clinical and animal studies have shown that EIM has the ability to detect changes in muscle composition and structure in a variety of neuromuscular diseases, including SMA, amyotrophic lateral sclerosis (ALS), myopathy, and radiculopathy [7-10].

In order to better understand the relationship between the surface measurements and the pathological alterations in tissue, we have been modeling neuromuscular disease to assess relationships between tissue histology, the electrical properties of the tissue (the tissue's conductivity and permittivity) and the surface measurements [11]. One important tool for this work is the finite element method (FEM); using a basic model of a limb and the measurement of electrical properties of the tissue, we can then attempt to predict the surface recorded voltages [12]. Such an approach is conceptually appealing for two reasons. First, FEM can take into account both intrinsic and geometric properties of the muscle. Second, we can also account for changes in limb shape, girth and subcutaneous fat. By altering our models, we can gain insight into how changes in muscle and non-muscular structures (e.g., subcutaneous fat) impact our results surface recorded data.

Ideally, we would like to perform analogous modeling in humans. Whereas it is straightforward to create a finite element model based on basic human anatomic data, obtaining human muscle to perform measurements of muscle conductivity and permittivity is considerably more difficult for both practical and ethical reasons. However, one initial approach would be to obtain conductivity and permittivity data on animals (both healthy and diseased) and input that data into the human model. Whereas this approach is not ideal, it certainly can provide an initial proof of principle as to how the inherent electrical properties of the muscle influence the surface recorded data.

Thus, in this initial analysis, we develop a single model of the upper arm based on data from two children, one with SMA and one healthy, who have nearly identical arm

Manuscript received March 18, 2011. This work was supported by the National Institutes of Health under Grant R01NS055099 and the Spinal Muscular Atrophy Foundation.

M. J., J. L., A. J. S., and M. S. are with Beth Israel Deaconess Medical Center, Department of Neurology, Boston, MA 02215 USA.

B. T. D. is with Children's Hospital Boston, Department of Neurology, Boston, MA 02215 USA (e-mail basil.darras@childrens.harvard.edu).

S. B. R. is with Beth Israel Deaconess Medical Center, Department of Neurology, Boston, MA 02215 USA (phone: 617-667-8130; fax: 617-667-3175; e-mail: srutkove@bidmc.harvard.edu)

morphology and who have undergone surface EIM measurements as part of our recently completed study [7]. We then input the permittivity and conductivity data from a group of healthy rats and a second group with another disease causing similar muscle pathology, amyotrophic lateral sclerosis (ALS), to evaluate how well the modeled data predict the surface measurements.

II. Methods

A. Approvals

The institutional review board of Children's Hospital Boston approved all the clinical methods of the study. Written consent was obtained from subjects over the age of 18, while subjects under the age of 18 provided either verbal or written assent in addition to written parental consent. All animal work was approved by the institutional animal care and use committee of Beth Israel Deaconess Medical Center.

B. Human Subjects

EIM was performed by placing four electrodes (Disposable Ring Electrodes, Carefusion, Middleton, WI) cut to quarter-length along the bulk of the biceps. Two inner voltage electrodes were placed 3 cm from the approximate center point of the muscle on either side along the length of the muscle, and the outer current electrodes placed 2 cm distal peripheral to the voltage electrodes. Standard clinical tape was used to reinforce electrode adhesion.

EIM measurements were recorded using Impedimed's Imp SFB7® device (Impedimed, San Diego, CA). This device measures resistance (R) and reactance (X) at frequencies ranging from 2 kHz to 1MHz. The third parameter, phase (θ) was then computed from the resulting reactance and resistance data [$\theta = \arctan(X/R)$], and the three parameters R, X, and θ were plotted against frequency.

Subcutaneous fat thickness was measured using ultrasound (Terason 2000, Teratech, Burlington, MA), where the probe was placed over the reference point of the muscle. If it was difficult to distinguish between fat and muscle in the resulting image, the subject was asked to contract and relax his or her muscle to better determine the fat-muscle interface. Muscle girth measurements were obtained by wrapping a measuring tape around the approximate mid-point of the bulk of the relaxed muscle.

From the total group of twenty-one healthy subjects and twenty-nine patients with genetically confirmed SMA who enrolled, two individuals of comparable age (approximately 8 years) and with nearly identical upper extremity morphology, including a subcutaneous fat thickness of 0.4 cm, girth of 18 cm, and muscle thickness of 2.5 cm were selected, from which a single model would be developed.

C. Animals

Five male SOD1 G93A amyotrophic lateral sclerosis rats were obtained from Taconic Laboratories (Germantown, NY); animals were sacrificed when they lost the ability to effectively feed themselves (as determined by complete paralysis of both the fore or hind limbs), at which point they were euthanized. The hind limb was then dissected and gastrocnemius muscle removed. Five healthy Wistar rats of approximately 18 weeks of age were similarly sacrificed and muscle tissue obtained in an identical fashion.

Immediately after sacrifice, longitudinal and transverse impedance measurements were taken over a frequency range of 0.5-1 MHz on a slab of the extracted gastrocnemius muscle as described in a custom impedance-measuring cell [11]. Given the friable nature of the ALS rat tissue, only longitudinal measurements (i.e., with current flow parallel to the muscle fibers) could be obtained The dielectric measurements, conductivity (σ) and relative permittivity (ε_r), were computed via the equations $\sigma = KG$, and $\varepsilon_r = KC/\varepsilon_0$, where: K is the geometry factor, given by the ratio of d, the distance between the two voltage electrodes and A, the cross-sectional area of the muscle; G is the conductance, given by $G = R/(R^2 + X^2)$; C is the capacitance, given by $C = X/\omega(R^2 + X^2)$; and ε_0 is the permittivity of free space. In other words, final computations were done according to equations (1) and (2):

$$(1)\ \sigma = \frac{d}{A} \cdot \frac{R}{R^2 + X^2};$$

$$(2)\ \varepsilon_r = \frac{1}{\varepsilon_0} \cdot \frac{d}{A} \cdot \frac{X}{\omega(R^2 + X^2)}$$

In all cases, A was computed using the height of the muscle and the 1×1 cm area of the muscle base.

An average value for both conductivity and permittivity for each group of animals was obtained and used in the FEM calculations that follow.

D. Finite Element Model Development

The model was developed and analyzed using Comsol Multiphysics software (Comsol, Inc, 4.1 Burlington, MA, AC/DC Module, Quasi-Statics [20]. The proximal end of the model extended toward the axilla and the distal end extended just proximal to the antecubital fossa (Fig 1). The model consisted of a skin-subcutaneous fat layer, a fascia layer, one bone (humerus) and several muscles: the biceps, the deltoid, and the triceps. Electrodes were based on the strip electrodes used in the actual EIM measurements, each measuring 0.8 cm by 2.4 cm. The voltage inter-electrode distance was set at approximately 6 cm; the outer current-emitting electrodes were placed 0.4 cm peripherally. Only the metallic surface of the electrode was modeled; no inter-electrode capacitances or contact impedances were included in the model (the latter is likely inconsequential being several orders of magnitude smaller than the input impedance of the voltage sensors). The muscle groups and tissue constituencies were consistent across the model. The final meshes for the model consisted of 59550 elements with 12s solution time. The normal

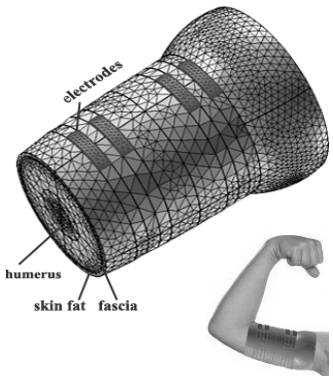

Fig. 1: Finite element model of human biceps constructed based on measurements from human subjects (below). The approximate muscle, bone, and surface structures are incorporated, though are not visible in this image. Mesh consists of 59550 tetrahedral elements.

component of the current between two adjoining tissue compartments was assumed to be continuous with no current flow out of any exterior boundaries, as the amount of current passing was likely to be small given the considerable distance from the array and the fact that both the elbow and axilla are bony and relatively poor conductors.

At each frequency, conductivity and permittivity values obtained from the rat muscle were incorporated into the model with the normal rat serving as the normal human and the ALS rat serving as the SMA data. Although both longitudinal and transverse dielectric data were obtained in the healthy rats, only longitudinal data were input into both models since only longitudinal data were available for the ALS animals. Skin-subcutaneous fat, fascia, and bone dielectric values were obtained over the frequency spectrum from Gabriel's dielectric survey and the associated online resources [13, 14]. Both skin-subcutaneous fat and fascia were assumed to be isotropic. The electrodes were assigned conductivity 5.0e5 S-m^{-1} and relative permittivity 1.

After solving the finite element problem, the voltage at the midpoint of both inner electrodes was assessed and the surface resistance and reactance values extracted. From these individual values, the phase was also calculated.

III. Results

The rat dielectric data (mean +/- standard error) are provided in Table 1 at selected frequencies. As can be seen, there are marked elevations in both conductivity and permittivity in the ALS animal muscle as compared to the healthy animal muscle. The actual human data (resistance and reactance) across the frequency spectrum are shown in Figure 2. Inputting the healthy and ALS animal values into the developed finite element model, we obtain two predicted data sets. The 50 kHz and peak phase data are summarized in Table 2 and the multi-frequency phase data in Figure 3. Although the predicted resistance is actually considerably lower than the actual value in SMA (due to the great increase in conductivity of the tissue), the predicted reactance drops even more dramatically, resulting in phase data that looks remarkably similar to that measured, although the peak frequencies are substantially off-set.

One concern with using these models is that the mesh number and granularity is somewhat arbitrary. Therefore it is helpful to verify that the same data input into a different mesh model would yield a similar result. Indeed, by decreasing the mesh from 59550 elements to 36431 elements, the parameters R, X, and θ change by only 4.9%, 9.7%, and 4.4%, respectively.

TABLE I
DIELECTRIC VALUES OF RAT MUSCLE AT SELECTED FREQUENCIES

	Normal		*ALS*	
Freq.	σ_L (Sm^{-1})	ε_L	σ_L (Sm^{-1})	ε_L
10000	0.24±0.017	155282±15029	2.50±0.508	788700±124302
25000	0.30±0.017	90853±7555	2.78±0.571	501394±35010
50000	0.37±0.016	54159±5249	3.13±0.570	342526±29989
100000	0.453±0.022	29731±2853	3.61±0.542	226492±24110
150000	0.503±0.028	19652±1360	3.92±0.51	166696±19717
300000	0.579±0.035	8552±941	4.58±0.433	99860±12531

Freq. Frequency (Hz)
σ_L longitudinal conductivity
ε_L longitudinal relative permittivity

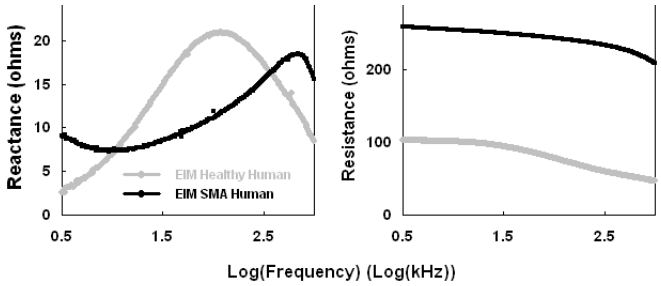

Fig. 2: Resistance and reactance data from the normal subject (gray) and the SMA patient (black) from 3 to 500 kHz.

TABLE II

COMPARISON OF EIM MEASURED VALUES WITH FEM MODEL PREDICTIONS

	EIM	
Value	**Normal**	**SMA**
R50	88.9 Ω	247 Ω
X50	18.1 Ω	9.7 Ω
P50	11.5 °	2.2 °
Peak Phase	16.6° (204 kHz)	4.8° (745 kHz)
	FEM	
Value	**Normal**	**SMA**
R50	98.4 ± 4.3 Ω	44.3 ± 2.0 Ω
X50	23.9 ± 6.4 Ω	3.1± 2.5 Ω
P50	13.6± 2.6 °	4.0 ± 2.3 °
Peak Phase	14.5° (22 kHz)	4.0° (47 kHz)

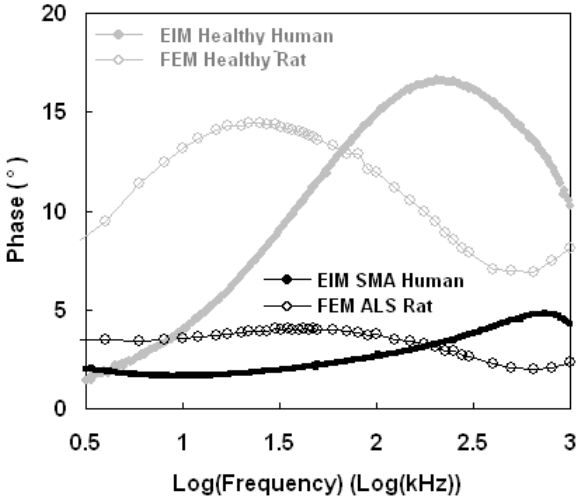

Fig. 3. Comparison of phase data for healthy human and model (gray) and disease human and model (black).

IV. Discussion

One of the challenges to the application of EIM in the assessment of neuromuscular disease is understanding how the surface measurements reflect muscle pathology. FEM provides one approach for studying this since directly measured electrical properties of the tissue can be input into a model to determine how closely those values correspond to the surface-measured ones. Ideally, to apply this most effectively to human beings, we would have fresh human muscle to measure. Since we could not obtain muscle for practical reasons, substituting animal muscle for human muscle provided a useful first approximation. Ideally, we would also use the same genetic model as the disease (in this case SMA); however, since such animal tissue was not available, we chose to use another severe degenerative disease characterized by motor neuron loss, namely ALS.

The "trick" of identifying two arms of nearly the same size, one diseased and one not, provided the possibility of creating a single model in which we could study the effects of differing dielectric data. The results were somewhat surprising. The diseased rat muscle had high conductivity, consistent with previous observations [11] but also a greatly elevated permittivity. These effects counteracted each other in the phase, in which peak values were remarkably close to that measured, although at displaced frequencies.

Both SMA and ALS share one important feature histologically: severe muscle fiber atrophy. However, in SMA, there is also substantial fibrosis and fatty infiltration of muscle, common findings in any longstanding neuromuscular disease. In the ALS rats, the pathological alterations develop only over several months, so less fibrosis and fatty infiltration are present. It is likely that these differences in muscle composition/structure impact the results. SMA mouse models have become available, but it is uncertain how well the muscle pathology mirrors the human condition.

Other limitations to this analysis include: 1. The permittivity and conductivity values were obtained from muscle measured *ex vivo*; despite measurements being performed shortly after sacrifice, some alteration in the actual impedance data is to be expected; 2. There were likely minor geometric differences between the two arms used to build the model that were ignored; 3. The values for the non-muscle components were taken from an online resource and could not be independently validated; 4. Since no transverse dielectric data could be obtained on the ALS rat muscle due to the tissue's friability, all these analyses are built from longitudinal permittivity and conductivity values only.

In summary, these results support the general prospect of using FEM as a means of assessing the impact of neuromuscular disease on human impedance data. Although the correspondence between the model and data is far from perfect, the overall trends are nonetheless promising. Future work will include obtaining human muscle in order to obtain more accurate dielectric data and attempts at inverse modeling to see how well surface measurements can predict muscle values both in animals and human subjects.

References

[1] M. R. Lunn, and C. H. Wang, "Spinal muscular atrophy," *Lancet,* vol. 371, no. 9630, pp. 2120-33, Jun 21, 2008.

[2] M. Oskoui, and P. Kaufmann, "Spinal muscular atrophy," *Neurotherapeutics,* vol. 5, no. 4, pp. 499-506, Oct, 2008.

[3] B. S. Russman, C. R. Buncher, M. White *et al.*, "Function changes in spinal muscular atrophy II and III. The DCN/SMA Group," *Neurology,* vol. 47, no. 4, pp. 973-6, Oct, 1996.

[4] P. Kaufmann, M. P. McDermott, B. T. Darras *et al.*, "Observational study of spinal muscular atrophy Type 2 and 3: Functional outcomes over one year," *Arch Neurol,* vol. (in press), 2011.

[5] K. J. Swoboda, T. W. Prior, C. B. Scott *et al.*, "Natural history of denervation in SMA: relation to age, SMN2 copy number, and function," *Ann Neurol,* vol. 57, no. 5, pp. 704-12, May, 2005.

[6] S. B. Rutkove, "Electrical impedance myography: Background, current state, and future directions," *Muscle Nerve,* vol. 40, no. 6, pp. 936-46, Dec, 2009.

[7] S. B. Rutkove, J. M. Shefner, M. Gregas *et al.*, "Characterizing spinal muscular atrophy with electrical impedance myography," *Muscle Nerve,* vol. 42, no. 6, pp. 915-21, Dec, 2010.

[8] S. Rutkove, G. Esper, K. Lee *et al.*, "Electrical impedance myography in the detection of radiculopathy," *Muscle Nerve,* vol. 32, pp. 335-341, 2005.

[9] S. B. Rutkove, H. Zhang, D. A. Schoenfeld *et al.*, "Electrical impedance myography to assess outcome in amyotrophic lateral sclerosis clinical trials," *Clin Neurophysiol,* vol. 118, no. 11, pp. 2413-8, Nov, 2007.

[10] A. Tarulli, G. Esper, K. Lee *et al.*, "Electrical impedance myography in the bedside assessment of inflammatory myopathy," *Neurology,* vol. 65, pp. 451-452, 2005.

[11] M. A. Ahad, P. M. Fogerson, G. D. Rosen *et al.*, "Electrical characteristics of rat skeletal muscle in immaturity, adulthood and after sciatic nerve injury, and their relation to muscle fiber size," *Physiol Meas,* vol. 30, no. 12, pp. 1415-27, Dec, 2009.

[12] L. L. Wang, M. A. Ahad, A. McEwan *et al.*, "Assessment of alterations in the electrical impedance of muscle after experimental nerve injury via finite element analysis," *Trans Biomed Engineering,* vol. (in press), 2011.

[13] C. Gabriel, S. Gabriel, and E. Corthout, "The dielectric properties of biological tissues: I. Literature survey," *Phys Med Biol,* vol. 41, no. 11, pp. 2231-49, Nov, 1996.

[14] "Institute of applied physics (IFAC). Dielectric properties of body tissues. 2007 [Online] Available: http://niremf.ifac.cnr.it/tissprop/.